



Published in final edited form as:

Nature. 2009 May 7; 459(7243): 113–117. doi:10.1038/nature07861.

CBP / p300-mediated acetylation of histone H3 on lysine 56

Chandrima Das¹, M. Scott Lucia², Kirk C. Hansen³, and Jessica K. Tyler^{1,*}

¹Department of Biochemistry and Molecular Genetics, University of Colorado School of Medicine

²Department of Pathology, University of Colorado School of Medicine

³Cancer Center Proteomics Core, University of Colorado School of Medicine

Abstract

Acetylation within the globular core domain of histone H3 on lysine 56 has recently been shown to play a critical role in packaging DNA into chromatin following DNA replication and repair in budding yeast 1, 2. However, the function or occurrence of this specific histone mark has not been studied in multi-cellular eukaryotes, mainly because the Rtt109 enzyme that is known to mediate acetylation of H3 K56 (H3 K56Ac) is fungal-specific 34. Here we demonstrate that in flies and humans the histone acetyl transferases CBP / p300 acetylate H3 K56, while Sir2 / hSirT1 / hSirT2 deacetylate H3 K56Ac. The histone chaperone Asf1 in *Drosophila*, Asf1a in humans, is required for acetylation of H3 K56 *in vivo*, while the histone chaperone CAF-1 is required for the incorporation of histones bearing this mark into chromatin. We show that in response to DNA damage, histones bearing acetylated K56 are assembled into chromatin in *Drosophila* and human cells, forming foci that colocalize with sites of DNA repair. Furthermore, acetylation of H3 K56 is elevated in multiple types of cancer, correlating with elevated levels of Asf1a in these tumors. Our identification of multiple proteins regulating the levels of H3 K56 acetylation in higher eukaryotes will allow future studies of this critical and unique histone modification that couples chromatin assembly to DNA synthesis, cell proliferation and cancer.

H3 K56 acetylation plays a critical role in regulating chromatin assembly following DNA synthesis 1, 2, chromatin disassembly during transcriptional activation 5 and cell survival 1 in yeast. Although H3 K56Ac clearly exists in *Drosophila* 6, 7, it is not known whether these functions of H3 K56Ac extend to multi-cellular eukaryotes. To investigate the function of H3 K56Ac in higher eukaryotes (Fig. S1), we asked whether histones carrying K56Ac are incorporated into chromatin following DNA repair in *Drosophila* S2 cells using antibodies specific to H3 K56Ac (Fig. S2). Exposure to hydroxyurea (HU), methyl methane sulfonate

Users may view, print, copy, and download text and data-mine the content in such documents, for the purposes of academic research, subject always to the full Conditions of use:http://www.nature.com/authors/editorial_policies/license.html#terms

Correspondence and requests for materials should be addressed to Jessica.tyler@uchsc.edu.

*Mail Stop 8101, PO Box 6511, Aurora CO 80045, jessica.tyler@uchsc.edu, Tel: 303-724-3224, Fax: 303-724-3221

Author contributions:

C.D. performed all the experiments, and devised some of the experiments. K.H. performed all the mass spectrometry analyses, M.S.L. performed all the pathology and IHC analyses, J.T. and C.D. wrote the manuscript and J.T. guided the research.

Author Information:

Reprints and permissions information is available at npg.nature.com/reprintsandpermissions.

Supplementary Information is linked to the online version of the paper at www.nature.com/nature. A figure summarizing the main results of this paper is also included as SI.

(MMS) or ultraviolet (UV) irradiation increased the level of H3 K56Ac on chromatin in a dose dependent manner, as determined by western blotting (Fig. 1a; Fig. S3) and immunofluorescence analyses (Fig. 1b, Fig. S4). Notably, these agents did not result in an accumulation of cells in S-phase (Fig. S5). Consistent with the requirement for the histone chaperone Anti-silencing function 1 (Asf1) for H3 K56 acetylation in yeast 8, we found that *Drosophila* Asf1 is required for both the endogenous level (Fig. 1c, S6) and the DNA damage-induced increase in the level (Fig. 1d) of H3 K56Ac *in vivo*. Strikingly, knockdown of another histone chaperone, chromatin assembly factor 1 (CAF-1), also drastically decreased the levels of H3 K56Ac on chromatin (Fig. 1e). However, knockdown of CAF-1, but not Asf1, resulted in accumulation of H3 K56Ac in the soluble protein fraction (Fig. 1f). As such, these results demonstrate that *Drosophila* CAF-1 is required for the assembly of histones carrying the K56Ac mark into chromatin, while Asf1 is required for H3 K56 acetylation *per se*. Using *Drosophila* embryos cycling synchronously between S and M phase, we detect no apparent difference in the amount of H3 K56Ac present in S or M phase nuclei (Fig. 1g). During mitosis, the staining of H3 K56Ac closely followed that of the condensed mitotic chromosomes suggesting that the H3 K56Ac mark is indeed on the chromatin rather than free in the nucleus. This is in stark contrast to the situation in yeast, where high levels of H3 K56Ac are only detectable in S-phase 9.

The enzymes that acetylate and deacetylate H3 K56 are unknown in multi-cellular organisms. Given the structural similarity between the yeast H3 K56 histone acetyltransferase (HAT) Rtt109 10 and CBP 11, we investigated the potential role of *Drosophila* CBP / Nejiro 12 in acetylating H3 K56. Treatment of S2 cells with curcumin – an inhibitor of the CBP/p300 family of HAT proteins 13 – drastically decreased H3 K56Ac levels (Fig. 2a). Furthermore, knockdown of CBP (Fig. 2b, Fig. S6), but not knockdown of another H3-specific HAT, Gcn5 14 (Fig. S6), blocked acetylation of H3 K56 in both the absence and presence of DNA damage (Fig. 2b,c), indicating that CBP is the major H3 K56 acetylase in *Drosophila*. Consistent with the idea that Asf1 and CBP function together to acetylate H3 K56 in flies, CBP coimmunoprecipitates with Asf1 (Fig. S7). The NAD-dependent histone deacetylases (HDAC) Hst3 and Hst4 are the major H3 K56Ac HDACs in yeast 15, 16. To investigate whether an NAD-dependent HDAC mediates H3 K56 deacetylation in *Drosophila*, we treated S2 cells with the NAD-dependent HDAC inhibitor nicotinamide 17. Nicotinamide, but not the related molecule nicotinic acid, resulted in increased H3 K56Ac levels (Fig. 2d, Fig. S8). Within the six *Drosophila* NAD-dependent HDACs, Sir2 is the closest counterpart of yeast Hst3/Hst4. Indeed, knockdown of *Drosophila* Sir2 greatly increased the level of H3 K56Ac (Fig. 2e, Fig. S6), indicating that Sir2 deacetylates H3 K56Ac in *Drosophila*.

Besides one global mass spectrometry study of histone modifications 18, H3 K56Ac has not previously been reported in human cells. By western blot analysis of chromatinized histones from HeLa cells, we clearly detected H3 K56Ac in humans (Fig. 3a). The amount of H3 K56Ac in HeLa and S2 cells was similar (Fig. S9), and mass spectrometry analysis confirmed the existence of H3 K56 acetylation in HeLa cells (Fig. S10). Furthermore, the amount of H3 K56Ac on chromatin increased in response to gamma-irradiation (IR), in a dose-dependent manner (Fig. 3a). The clear colocalization of H3 K56Ac and the

phosphorylated histone variant H2AX (H2AXp) following DNA damage indicated that the assembly of histones carrying H3 K56Ac is enriched at sites of DNA repair (Fig. 3b). The levels of H3 K56Ac on human chromatin were also increased following UV, MMS and HU treatment (Fig. 3c). By flow cytometry analysis, we found that even in the absence of DNA damage, human cells in all stages of the cell cycle have significant H3 K56Ac staining (Fig. S11).

Consistent with the reduced level of acetylation of H3 K56 in human cells upon curcumin treatment (Fig. S12), we found that both CBP and p300 contribute to acetylation of H3 K56 in human cells (Fig. 3d, e, Fig. S13). Furthermore, CBP and p300 directly acetylate histone H3 on lysine 56 *in vitro* (Fig. 3f, g), with high efficiency as determined by mass spectrometry analysis (Fig. S13). Acetylation of H3 K56Ac by the yeast HAT Rtt109 requires that histones H3-H4 be pre-bound to the histone chaperone Asf1 19. However, this is not the case with CBP *in vitro*, because it efficiently acetylated H3 K56 irrespective of whether the histones were bound to Asf1 (Fig. 3f). Towards identifying the human HDAC for H3 K56, we found that treatment of human cells with nicotinamide greatly increased the level of H3 K56Ac (Fig. 3h), implicating an NAD-dependent HDAC. siRNA knockdown analyses of SirT1 and SirT2 indicated that both enzymes contribute to deacetylation of H3 K56 in human cells (Fig. 3i). Indeed, both recombinant hSirT2 and hSirT1 deacetylated H3 K56 *in vitro*, with SirT2 being the more active enzyme (Fig 3j, Fig S14). Treatment of human cells with sodium butyrate drastically increased H3 K56Ac levels (Fig. S12), additionally implicating a class I or class II HDAC in H3 K56 deacetylation. Taken together, these data reveal that human CBP / p300 are the H3 K56 acetylases while hSirT2 and hSirT1 are H3 K56Ac deacetylases.

Next, we investigated whether either of the two forms of the human Asf1 histone chaperone, Asf1a and Asf1b, are involved in H3 K56 acetylation. Using yeast strains that express equivalent levels of human Asf1a, human Asf1b or *Drosophila* Asf1 in the place of the yeast Asf1 protein 20, it was apparent that human Asf1a and *Drosophila* Asf1, but not human Asf1b, can assist yeast Rtt109 in the acetylation of H3 K56 (Fig. 4a). In agreement, knockdown of Asf1a decreased the amount of H3 K56Ac in human cells more than knockdown of Asf1b while the combined knockdown of both Asf1a and Asf1b resulted in no detectable H3 K56Ac (Fig. 4b). The requirement for human Asf1 for H3 K56 acetylation *in vivo*, but not *in vitro*, indicates that additional constraints exist *in vivo*. We also found that human Asf1 is required for the increase in levels of H3 K56Ac on chromatin following DNA damage, while human CAF-1 is required for the assembly of the H3 K56 acetylated histones onto DNA (Fig. 4c, d). Further supporting the role of Asf1a versus Asf1b in H3 K56 acetylation, there is a striking correlation between levels of H3 K56 acetylation and Asf1a but not Asf1b in a wide variety of normal and cancerous human tissues (Fig. 4e). The increase in levels of H3 K56Ac in many cancer tissues (Fig. 4e, Fig. S15, Fig. S16) in a manner that is proportional to tumor grade (Fig. S17, Table S1) led us to investigate whether H3 K56Ac levels correlate with proliferation and / or tumorigenicity. Non-tumorigenic MCF10A cells show much lower levels of H3 K56Ac than tumorigenic MCF7 cells derived from the same breast tumor (Fig. 4f). Furthermore, H3 K56Ac staining also occurred in cancer cells that are not positive for the proliferation marker Ki-67 21 (Fig. 4g). These data

suggest that H3 K56Ac levels correlate with tumorigenicity rather than proliferation. Consistent with the elevated level of H3 K56Ac in dedifferentiated cancer cells, we also find that H3 K56Ac levels positively correlate with the undifferentiated nature of cells. For example, H3 K56Ac levels are higher in embryos than cell lines (Fig. 4h) and the level of H3 K56Ac rapidly drops upon in vitro differentiation of cell lines (Fig. 4i, Fig. S18).

Recent yeast studies indicate that H3 K56Ac increases the ability of histones to bind to CAF-1, which subsequently deposits the histones onto newly synthesized DNA 1, 2. This is likely to also be the case in higher eukaryotes, given that knockdown of CAF-1 blocks incorporation of H3 K56Ac into chromatin (Fig. 1F, 4D) and that inhibition of Asf1 blocks DNA replication and chromatin assembly of newly-synthesized DNA 22–24. In agreement, CBP/p300 promote DNA replication and cell proliferation 2526. Furthermore, p300 is recruited to sites of DNA synthesis via its interaction with PCNA 27, consistent with a direct role for CBP/p300 in promoting chromatin assembly via K56 acetylation after DNA synthesis. It is also intriguing that the HAT activity of human CBP is highest at the G₁/S boundary - the time at which massive amounts of newly-synthesized H3 is produced to assemble the newly-replicated genomes into chromatin 28. We propose that the CBP/p300-mediated acetylation of H3 K56 promotes the subsequent assembly of newly-synthesized DNA into chromatin in higher eukaryotes (Fig. S1); the inhibition of which negatively feeds back to block DNA replication and cell proliferation. Given that the H3 K56Ac mark is rapidly removed by histone deacetylases after histone incorporation onto newly-replicated DNA in yeast 15, 16, it will be interesting to determine whether the H3 K56ac deacetylation process is defective in undifferentiated and dedifferentiated cancer cells. Alternatively, the elevated levels of H3 K56Ac in cancer cells and undifferentiated cells may reflect hyperdynamic exchange of histones 29 in undifferentiated cells that is lost upon differentiation.

Methods Summary

Yeast Strains and Tissue Culture

Genotypes of strains and tissue culture details are described in the supplemental material.

Histone Isolation and Western Blotting

Histone extraction was performed as described previously 30. Briefly, following nuclear pellet isolation, soluble chromatinized histones were extracted with 0.4 M and 0.25 M HCl, for S2 cells and HeLa cells respectively, followed by TCA precipitation. NP40-induced extraction of detergent soluble proteins is detailed in the supplemental methods. Briefly, following treatment with 0.1% NP40 for 10 mins, centrifugation at 3000 rpm for 10 mins lead to the separation of supernatant and pellet fractions. Antibody details are provided in the supplemental methods.

Immunofluorescence

Immunofluorescence following 0.5% triton-X extraction was performed as described previously 23.

RNAi

Knockdowns were performed in S2 cells as described previously 23. Briefly, dsRNA was generated by in vitro transcription using the Megascript kit from Ambion. After testing the quality of each dsRNA, it was transfected into S2 cells for different length of time to ensure complete silencing of the gene of interest, as determined by western blotting. Primer sequences are available upon request. SiRNA for silencing in HeLa cells were obtained from Dharmacon.

HAT and HDAC assays

Recombinant CBP, p300, SirT1 and SirT2 were obtained from Biomol. Following a 10 min preincubation of HAT with either purified recombinant Asf1-H3H4 complexes, purified *Drosophila* core histones or H3-H4 tetramers at 30°C, Acetyl-CoA was added and incubated at 30°C for 10 mins, followed by TCA precipitation. HDAC assays: following acetylation of H3 K56 by CBP/p300, curcumin was added to inhibit CBP/p300 and the histones carrying H3 K56Ac were incubated with SirT1 or SirT2 in the presence of NAD at 30°C for the indicated length of time.

Methods

Yeast strains

The “No Asf1” yeast strain is ROY1170; *MAT* alpha *ade2-1 LYS2 leu2-3, 112 his3-11trp1-1 ura3-1 asf1::his5+ TELVIII::URA3 HMRA::ADE2 can1-10031*

The “yAsf1” strain is ROY1172; *MAT* alpha *ade2-1 LYS2 leu2-3, 112 his3-11 trp1-1 ura3-1 TELVIII::URA3 HMRA::ADE2 can1-10031*

The “dAsf1” is BAT014; *MAT* alpha *ade2-1 leu2-3, 112 his3-11 trp1-1 ura3-1 TEVIII::URA HMRA::ADE2 asf1::dAsf1-13myc KAN20*

The “hAsf1a” strain is BAT016; *MAT* alpha *ade2-1 leu2-3, 112 his3-11 trp1-1 ura3-1 TEVIII::URA HMRA::ADE2 asf1::hAsf1a-13myc KAN20*

The “hAsf1b” strain is KDY006 *MAT* alpha *ade2-1 leu2-3, 112 his3-11 trp1-1 ura3-1 TEVIII::URA HMRA::ADE2 asf1::hAsf1b-13myc KAN20*

Tissue culture media

Drosophila S2 cells were maintained in Schneider’s media supplemented with 10% FBS at 30°C. HeLa cells were grown in DMEM media supplemented with 10% FBS at 30°C in 5% CO₂ supply. Unless otherwise stated, curcumin was used at 100 µM for 24 hours, nicotinamide, nicotinic acid or sodium butyrate were used at 25 mM for 12 hours. SHSY-5Y cells were grown in media constituted with 50% Ham’s F12 and 50% MEM, supplemented with 10%FBS at 30°C in 5% CO₂ supply. SHSY-5Y cells were treated with 0.02 mM Retinoic acid for 3 to 6 days to induce differentiation. MCF7 cells were grown in DMEM supplemented with 10% FBS at 30°C in 5% CO₂ supply. MCF10A cells were grown in DMEM supplemented with 10% FBS, 0.01 mg/ml insulin, 0.5 µg/ml hydrocortisone, 0.02

µg/ml EGF and 0.1 µg/ml cholera toxin. For trypsinization, 0.05% Trypsin-EDTA for MCF10A/12A, 0.25 % Trypsin-EDTA for rest of the cell lines were used.

Antibodies and commercial blots

Drosophila H3 K56Ac was detected using an H3 K56Ac specific antibody from Upstate (Catalogue No 07–677) while human H3 K56Ac was detected using a rabbit monoclonal H3 K56Ac specific antisera from Epitomics (Catalogue No 2134–1). Gcn5 was detected with an antibody from Abcam (Catalogue No ab52787), total H3 was detected with an antibody from Abcam (Catalogue No ab1791), H3K9Ac was detected with an antibody from Upstate (Catalogue No 07–352), human CBP was detected with an antibody from Abcam (Catalogue No ab2832), human p300 was detected with an antibody from Abcam (Catalogue No ab61217). Asf1 was detected with a previously described antibody 32. The anti-phospho H2AX antibody was from Upstate (Catalogue No 07–164). Commercial tissue blots, having normal and cancerous samples were procured from G Biosciences (TB56 Set I, II). These blots contain lysates (in a denaturing buffer supplemented with a cocktail of protease inhibitors to minimize proteolytic degradation) extracted from human normal and tumor tissues. Equal amounts of proteins were loaded on a 4–20% gradient denaturing PAGE, followed by transfer in a PVDF membrane.

Isolation of pellet and supernatant fractions

NP40-induced extraction of detergent soluble proteins was performed as described elsewhere 33. Briefly, following treatment with 0.1 or 0.5% NP40, for 10 mins, centrifugation at 3000 rpm for 10 mins lead to the separation of non-chromatin supernatant and chromatin pellet fractions. The pellet fractions were subsequently purified and analyzed by western blotting for the presence of H3K56Ac. Sup (non-chromatin) and pellet (chromatin) fractions were resolved following 0.1% NP40 treatment as mentioned elsewhere 34.

Isolation of histones from drosophila embryos

The histone extraction from stage 9–13 drosophila embryos was performed as per standard protocol 35. Briefly, the embryos were homogenized in lysis buffer (15 mM Tris, pH 7.5, 60 mM KCl, 15 mM NaCl, 3 mM EDTA, 0.1 mM EGTA, 0.15 mM Spermine, 0.5 mM Spermidine, 0.2% NP40, 10 mM NaF and protease inhibitors) supplemented with a cocktail of HDAC inhibitors. The nuclear pellet was subsequently treated with 0.4M HCL for 1 hr for histone extraction. The extracted histones were subsequently TCA precipitated and analyzed for the H3K56 acetylation levels.

Immunoprecipitation

S2 whole cell extracts were prepared using RIPA buffer (150 mM NaCl, 1% NP40, 0.5% NaDeoxycholate, 0.1% SDS, 50 mM Tris, pH 8, 10 mM NaF, 0.4 mM EDTA, 10% Glycerol and protease inhibitors) supplemented with protease inhibitors. The pre-blocked protein G-sepharose bound dAsf1 antibody was then incubated with whole cell extracts. Following extensive washes, the bead bound protein complexes were analyzed by western blotting using dCBP/H3 antibodies.

RNAi in human cells

siRNA transfections were carried out in HeLa cells using INTERFERin Polyplus (409–10) as per the standard protocol. The different siRNA sequences chosen were synthesized from Dharmacon used elsewhere:

CAF1 (p150)-1: 5' AGGGGAAAGCCGAUGACAU (dTdT)-3' 36

Asf1a: 5'-AAGUGAAGAAUACGAUCAAGU (dTdT)-3' 22

Asf1b: 5'-AACAAACGAGUACCUCAACCCU (dTdT)-3' 22

SirT1: 5'-ACUUUGCUGUAACCCUGUA (dTdT)-3' 37

SirT2: ON-TARGETplus SMARTpool L-004826 (from Dharmacon)

CBP: 5'-CGGCACAGCCUCUCAGUCA (dTdT)-3' 38

p300: 5'-UGACACAGGCAGGCUU GAC UU-3' 39

For CAF1 and Asfa/b, the siRNA transfection time was for 48 hrs. For CBP, p300, SirT1, and SirT2, the transfection time was 72 hrs.

Flow cytometry

After the different treatments, the cells were washed with PBS and subject to Ethanol fixation for at least 1 hour. The cells were then Triton extracted (0.05%), blocked in 1% BSA, and stained with H3K56Ac antibody (Epitomics) at 1:250 dilution for 1 hour. After extensive washing in PBST, the cells were put in Alexa 568 conjugated secondary antibody for 1 hour at 1:1000 dilution. The cells were extensively washed, 0.5 mg/ml RNase treated and finally stained with propidium iodide at 10ug/ml final concentration for 1 hr in dark. The cell cycle stages and K56ac staining intensities were then measured by flow cytometry.

Immunohistochemistry (IHC)

After deparafinizing, slides were rinsed in ethanol. Antigen retrieval was performed with 10 mM Sodium Citrate for 5 mins at 22 psi. The staining was performed with the I-VIEW enhanced DAB Kit. Counterstaining was with Mayer's Hematoxylin and the mounting media used was Cytoseal 60. IMH-346 and IMT-01233 tissue array slides were procured from Imgenex. Additional slides for normal and tumor skin, thyroid, cerebellum, colon, larynx, ovary tissues were analyzed from the UCCC Pathology core. Each of the sample specimens was pathologically confirmed before carrying out the immunohistochemistry.

DNA damaging treatments

Unless otherwise indicated, 0.05% MMS and 150 mM HU treatment was performed for 12 hours, 49,995 J/m² of UV or 1, 1.25, and 1.5 Gray gamma irradiation were given to visualize the damage foci.

Immunofluorescence

Briefly, following 4% formaldehyde fixation, cells were permeabilized by 0.5% Triton X 100, blocked in 1% BSA, and treated with primary antibody followed by Alexa 488 conjugated secondary antibody. Vectashield mounting medium containing DAPI was used for DNA staining. H3 K56Ac and H2AXp antibodies were detected using Alexa 488 or Alexa 568 conjugated secondary antibody, respectively, following previously described methods 32.

Mass spectrometry analysis

Histone K56 Acetylation Analysis by Mass Spectrometry

Sample digestion—A standard in-gel digestion protocol was used based on the method of Rosenfeld *et al.* 40 and Hellman *et al.* 41 Iodoacetamide (IAM) was used for Cys alkylation.

Liquid Chromatography – tandem mass spectrometry data acquisition—

Digests were analyzed on a LTQ-ICR hybrid mass spectrometer (LTQ-FT Ultra, Thermo Fisher, San Jose, CA). Peptide desalting and separation was achieved using a dual capillary/nano pump HPLC system (Agilent 1200, Palo Alto, CA). On this system 8 μ L of sample was loaded onto a trapping column (ZORBAX 300SB-C18, dimensions 5 \times 0.3 mm 5 μ m; Agilent Technologies, Santa Clara, CA) and washed with 5% ACN, 0.1% FA at a flow rate of 15 μ L/min for 5 minutes. At this time the trapping column was put online with the nano-pump at a flow rate of 350 nL/min. An 80 minute gradient from 8% ACN to 32% ACN was used to separate the peptides. The column was made from an in-house pulled 360/100 nm (outer/inner diameter) fused silica capillary using a model P-2000 laser puller (Sutter Instrument Co.; Novato, CA). The column was packed 15 cm in length with Jupiter C18 resin (Phenomenex; Torrance, CA). The column was kept at a constant 40°C using an in-house built column heater. The column effluent was coupled directly to the mass spectrometer with an in-house built nanospray ion source. Data acquisition was performed using the instrument supplied Xcalibur (version 2.0.7) software. The 90 minute LC runs were monitored by sequentially recording the precursor scan (MS) followed by three collision-induced dissociation (CID) acquisitions (MS/MS). Normalized collision energies were employed using helium as the collision gas. MS survey scans were acquired in the ICR cell at a resolution of 25,000 at 400 m/z. After two acquisitions of a given ion within 45 seconds, the ion was excluded for 150 seconds.

Data analysis—The manufacture supplied extract_msn script was used to create de-isotoped, centroided peak lists from the raw spectra (.mgf format). These peak lists were searched against the SwissProt database (v54.8) using Mascot™ server (Version 2.2, Matrix Science). For searches mass tolerances were \pm 10 ppm for MS peaks, and \pm 0.6 Da for MS/MS fragment ions. Trypsin specificity was used allowing for 1 missed cleavage. The modifications of Met oxidation, protein N-terminal acetylation, peptide N-terminal pyroglutamic acid formation (Q), lysine acetylation and lysine mono-, di- and tri-methylation were allowed for. Peptides were required to reach a score of 6 and proteins were filtered at a significance of $P < 0.005$ and requiring bold red hits (top match for a given spectrum).

Semiquantitation of K56 acetylation—The tryptic peptide resulting from the unacetylated K56 form of H3 was “K.STELLIR.K”. This peptide was compared to the tryptic peptide resulting from the K56 acetylated form of H3 “R.YQ-AcK-STELLIR.K”. Trypsin cleavage does not occur on the C-terminal side of acetylated K56 due to the loss of the positive charge. Extracted ion chromatograms were calculated for the range m/z 416.23–416.27 for the “STELLIR” peptide. It was confirmed that the peak from ~27–30 minutes corresponded to the “STELLIR” peptide, based on assignment of several CID spectra. Likewise the extracted ion chromatogram from 646.81–646.91 was used to calculate the acetylated form of the peptide. The identification of this peak was also confirmed by several redundant CID spectra. Peak areas were calculated using the “Genesis” Algorithm from within the Bioworks Qual Browser (version 2.0, Thermo Fisher). The data is stated as the percentage of K56Ac with respect to total K56 and K56Ac.[A1] While this isn’t a direct measure of percentage acetylation it does show that K56Ac increases and accordingly K56 decreases. Note that our analyses do not distinguish among the three different histone variants: H3.3 vs H3.1 vs H3.2.

Verification of H3 K56 acetylation rather than H3 K56 trimethylation—Note that we can readily distinguish the acetylated lysine 56 and trimethylated lysine 56 by mass using our analytical platform. The mass difference between acetylation (H_2C_2O , 42.01056 Da) and tri-methylation (H_6C_3 , 42.04695 Da) of the peptide in question can readily be distinguished using the FT-ICR instrument where we routinely measure ions at less than 1 ppm mass accuracy. The average parent ion error for H3 was -0.66 ppm and $3*\text{StdDev}$ (3σ) of all the assigned peptides was 1.26 ppm. The mass error for the ion used to assign YQK(Ac)STELLIR from the in vitro derived sample had a mass error of -0.74 ppm whereas the mass error for the tri-methylated form would have been -28.9 ppm; well outside the acceptable error tolerance for the mass spectrometer used and observed for the rest of the peptide assignments. Similarly the mass error for assignment of the peptide YQK(Ac)STELLIR from the in vivo samples was -1.7 ppm, and the error if this precursor would be assigned as the tri-methylated form would be an unacceptable -29.8 ppm.

Supplementary Material

Refer to Web version on PubMed Central for supplementary material.

Acknowledgements

We thank Jim Kadonaga for *Drosophila* embryos and Sir2 antibody, Alexander Mazo for the CBP antisera and Eric Nigg for Asf1a/b antisera. We thank Candice Wike and the UC microscope core, and the UCCC flow cytometry core for assistance. This work was supported by funding from the National Institutes of Health (grants GM64475 and CA95641) to JKT.

References

1. Chen CC, et al. Acetylated lysine 56 on histone H3 drives chromatin assembly after repair and signals for the completion of repair. *Cell*. 2008; 134:231–243. [PubMed: 18662539]
2. Li Q, et al. Acetylation of histone H3 lysine 56 regulates replication-coupled nucleosome assembly. *Cell*. 2008; 134:244–255. [PubMed: 18662540]

3. Han J, et al. Rtt109 acetylates histone H3 lysine 56 and functions in DNA replication. *Science*. 2007; 315:653–655. [PubMed: 17272723]
4. Xhemalce B, et al. Regulation of histone H3 lysine 56 acetylation in *Schizosaccharomyces pombe*. *J Biol Chem*. 2007; 282:15040–15047. [PubMed: 17369611]
5. Williams SK, Truong D, Tyler JK. Acetylation in the globular core of histone H3 on lysine-56 promotes chromatin disassembly during transcriptional activation. *Proc Natl Acad Sci U S A*. 2008; 105:9000–9005. [PubMed: 18577595]
6. Xu F, Zhang K, Grunstein M. Acetylation in histone H3 globular domain regulates gene expression in yeast. *Cell*. 2005; 121:375–385. [PubMed: 15882620]
7. Schneider J, Bajwa P, Johnson FC, Bhaumik SR, Shilatfard A. Rtt109 is required for proper H3K56 acetylation: a chromatin mark associated with the elongating RNA polymerase II. *J Biol Chem*. 2006; 281:37270–37274. [PubMed: 17046836]
8. Recht J, et al. Histone chaperone Asf1 is required for histone H3 lysine 56 acetylation, a modification associated with S phase in mitosis and meiosis. *Proc Natl Acad Sci U S A*. 2006; 103:6988–6993. [PubMed: 16627621]
9. Masumoto H, Hawke D, Kobayashi R, Verreault A. A role for cell-cycle-regulated histone H3 lysine 56 acetylation in the DNA damage response. *Nature*. 2005; 436:294–298. [PubMed: 16015338]
10. Tang Y, et al. Fungal Rtt109 histone acetyltransferase is an unexpected structural homolog of metazoan p300/CBP. *Nat Struct Mol Biol*. 2008; 15:738–745. [PubMed: 18568037]
11. Liu X, et al. The structural basis of protein acetylation by the p300/CBP transcriptional coactivator. *Nature*. 2008; 451:846–850. [PubMed: 18273021]
12. Florence B, McGinnis W. A genetic screen of the *Drosophila* X chromosome for mutations that modify Deformed function. *Genetics*. 1998; 150:1497–1511. [PubMed: 9832527]
13. Marcu MG, et al. Curcumin is an inhibitor of p300 histone acetyltransferase. *Med Chem*. 2006; 2:169–174. [PubMed: 16787365]
14. Carre C, Szymczak D, Pidoux J, Antoniewski C. The histone H3 acetylase dGcn5 is a key player in *Drosophila melanogaster* metamorphosis. *Mol Cell Biol*. 2005; 25:8228–8238. [PubMed: 16135811]
15. Celic I, et al. The sirtuins hst3 and Hst4p preserve genome integrity by controlling histone h3 lysine 56 deacetylation. *Curr Biol*. 2006; 16:1280–1289. [PubMed: 16815704]
16. Maas NL, Miller KM, DeFazio LG, Toczyski DP. Cell cycle and checkpoint regulation of histone H3 K56 acetylation by Hst3 and Hst4. *Mol Cell*. 2006; 23:109–119. [PubMed: 16818235]
17. Francis NJ, Kingston RE. Mechanisms of transcriptional memory. *Nat Rev Mol Cell Biol*. 2001; 2:409–421. [PubMed: 11389465]
18. Garcia BA, et al. Organismal differences in post-translational modifications in histones H3 and H4. *J Biol Chem*. 2007; 282:7641–7655. [PubMed: 17194708]
19. Tsubota T, et al. Histone H3-K56 acetylation is catalyzed by histone chaperone-dependent complexes. *Mol Cell*. 2007; 25:703–712. [PubMed: 17320445]
20. Tamburini BA, Carson JJ, Adkins MW, Tyler JK. Functional conservation and specialization among eukaryotic anti-silencing function 1 histone chaperones. *Eukaryot Cell*. 2005; 4:1583–1590. [PubMed: 16151251]
21. Scholzen T, Gerdes J. The Ki-67 protein: from the known and the unknown. *J Cell Physiol*. 2000; 182:311–322. [PubMed: 10653597]
22. Groth A, et al. Human Asf1 Regulates the Flow of S Phase Histones during Replicational Stress. *Mol Cell*. 2005; 17:301–311. [PubMed: 15664198]
23. Schulz LL, Tyler JK. The histone chaperone ASF1 localizes to active DNA replication forks to mediate efficient DNA replication. *Faseb J*. 2006
24. Sanematsu F, et al. Asf1 is required for viability and chromatin assembly during DNA replication in vertebrate cells. *J Biol Chem*. 2006
25. Ait-Si-Ali S, et al. CBP/p300 histone acetyl-transferase activity is important for the G1/S transition. *Oncogene*. 2000; 19:2430–2437. [PubMed: 10828885]

26. Yao TP, et al. Gene dosage-dependent embryonic development and proliferation defects in mice lacking the transcriptional integrator p300. *Cell*. 1998; 93:361–372. [PubMed: 9590171]
27. Hasan S, Hassa PO, Imhof R, Hottiger MO. Transcription coactivator p300 binds PCNA and may have a role in DNA repair synthesis. *Nature*. 2001; 410:387–391. [PubMed: 11268218]
28. Ait-Si-Ali S, et al. Histone acetyltransferase activity of CBP is controlled by cycle-dependent kinases and oncoprotein E1A. *Nature*. 1998; 396:184–186. [PubMed: 9823900]
29. Meshorer E, et al. Hyperdynamic plasticity of chromatin proteins in pluripotent embryonic stem cells. *Dev Cell*. 2006; 10:105–116. [PubMed: 16399082]
30. Shechter D, Dormann HL, Allis CD, Hake SB. Extraction, purification and analysis of histones. *Nat Protoc*. 2007; 2:1445–1457. [PubMed: 17545981]
31. Tyler JK, et al. The RCAF complex mediates chromatin assembly during DNA replication and repair. *Nature*. 1999; 402:555–560. [PubMed: 10591219]
32. Tyler JK, et al. Interaction between the Drosophila CAF-1 and ASF1 Chromatin Assembly Factors. *Mol Biol Cell*. 2001; 21:6574–6584.
33. Frei C, Gasser SM. The yeast Sgs1p helicase acts upstream of Rad53p in the DNA replication checkpoint and colocalizes with Rad53p in S-phase-specific foci. *Genes Dev*. 2000; 14:81–96. [PubMed: 10640278]
34. Pallier C, et al. Association of chromatin proteins high mobility group box (HMGB) 1 and HMGB2 with mitotic chromosomes. *Mol Biol Cell*. 2003; 14:3414–3426. [PubMed: 12925773]
35. Madigan JP, Chotkowski HL, Glaser RL. DNA double-strand break-induced phosphorylation of Drosophila histone variant H2Av helps prevent radiation-induced apoptosis. *Nucleic Acids Res*. 2002; 30:3698–3705. [PubMed: 12202754]
36. Hoek M, Stillman B. Chromatin assembly factor 1 is essential and couples chromatin assembly to DNA replication in vivo. *Proc Natl Acad Sci U S A*. 2003; 100:12183–12188. [PubMed: 14519857]
37. Kim EJ, Kho JH, Kang MR, Um SJ. Active regulator of SIRT1 cooperates with SIRT1 and facilitates suppression of p53 activity. *Mol Cell*. 2007; 28:277–290. [PubMed: 17964266]
38. Megiorni F, Indovina P, Mora B, Mazzilli MC. Minor expression of fascin-1 gene (FSCN1) in NTera2 cells depleted of CREB-binding protein. *Neurosci Lett*. 2005; 381:169–174. [PubMed: 15882811]
39. Kuninger D, et al. Gene disruption by regulated short interfering RNA expression, using a two-adenovirus system. *Hum Gene Ther*. 2004; 15:1287–1292. [PubMed: 15684704]
40. Rosenfeld J, Capdevielle J, Guillemot JC, Ferrara P. In-gel digestion of proteins for internal sequence analysis after one- or two-dimensional gel electrophoresis. *Anal Biochem*. 1992; 203:173–179. [PubMed: 1524213]
41. Hellman U, Wernstedt C, Gonez J, Heldin CH. Improvement of an "In-Gel" digestion procedure for the micropreparation of internal protein fragments for amino acid sequencing. *Anal Biochem*. 1995; 224:451–455. [PubMed: 7710111]

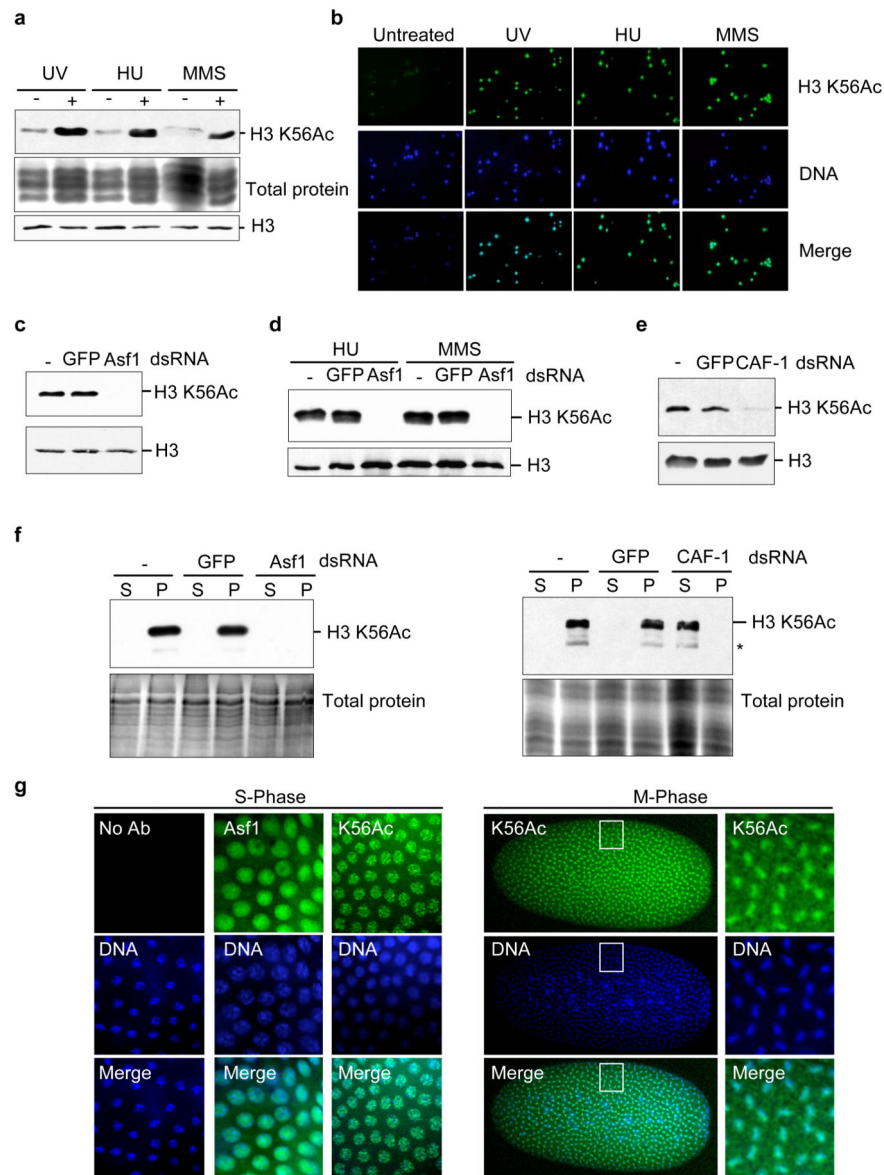


Figure 1. *Drosophila* Asf1 promotes H3 K56 acetylation, while CAF-1 deposits H3 K56Ac into chromatin

a and **b** H3 K56ac levels in chromatin after DNA damage. **c**. Asf1 is required for H3 K56 acetylation, and in response to DNA damage, **d**. **e**. H3 K56Ac levels on chromatin following CAF-1 p180 knockdown. **f**. H3 K56Ac levels in free histones in the supernatant (“S”) and chromatin bound pellet (“P”). * indicates a likely proteolytic product of H3. **g**. *Drosophila* embryos were stained with no primary antibody (“no Ab”), antisera to Asf1 or K56Ac, as indicated. Secondary antibody was included in all analyses

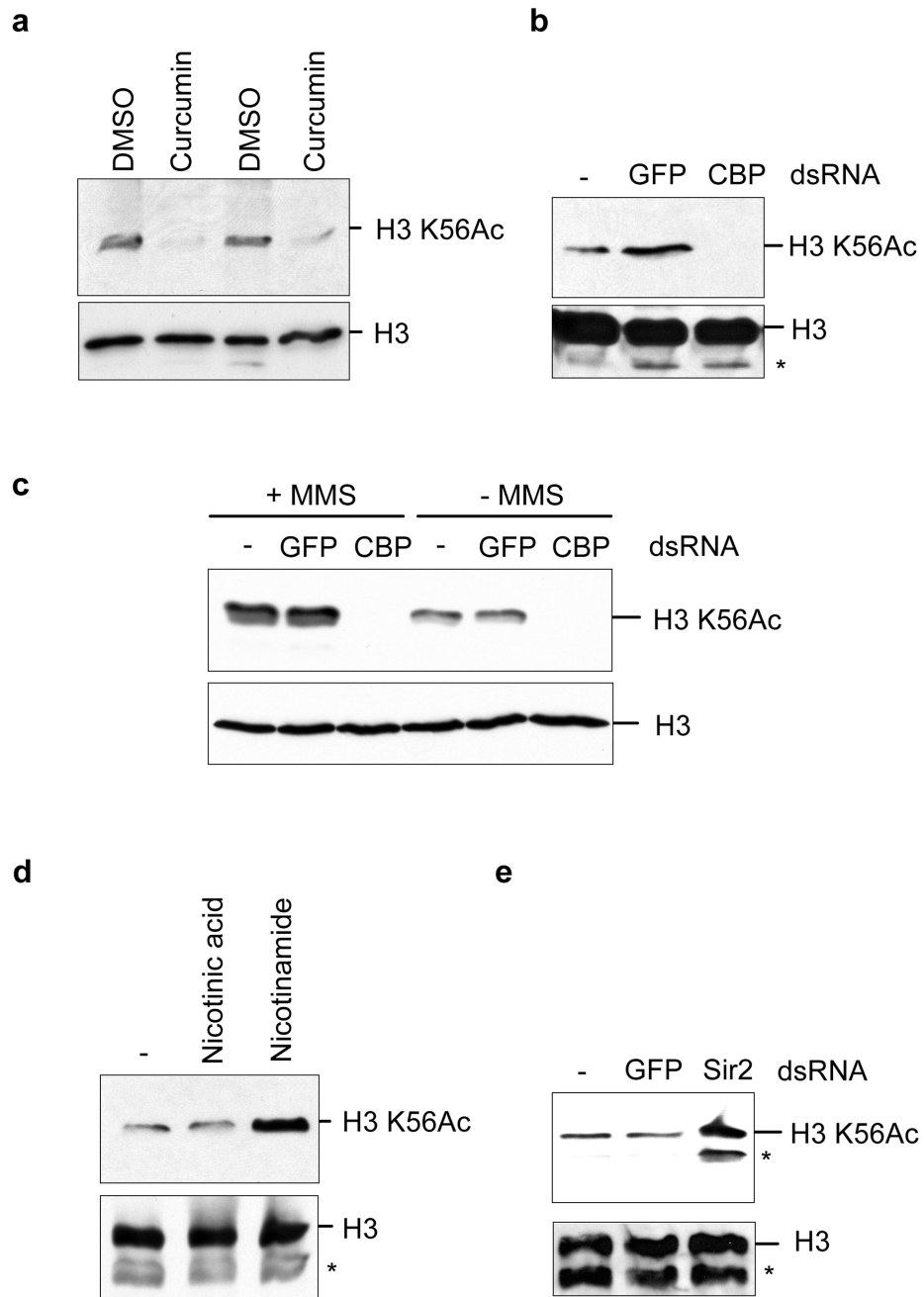


Figure 2. *Drosophila* CBP acetylates H3 K56, while Sir2 deacetylates H3 K56Ac in vivo
a. Inhibition of CBP by curcumin lowers levels of H3 K56Ac in S2 cells. Duplicate analyses are shown. **b.** CBP acetylates H3 K56. **c.** CBP is required for the increase of H3 K56Ac on chromatin after DNA damage. **d.** Inhibition of NAD-dependent HDACs by nicotinamide increases K56Ac. **e.** Sir2 deacetylates H3 K56Ac.

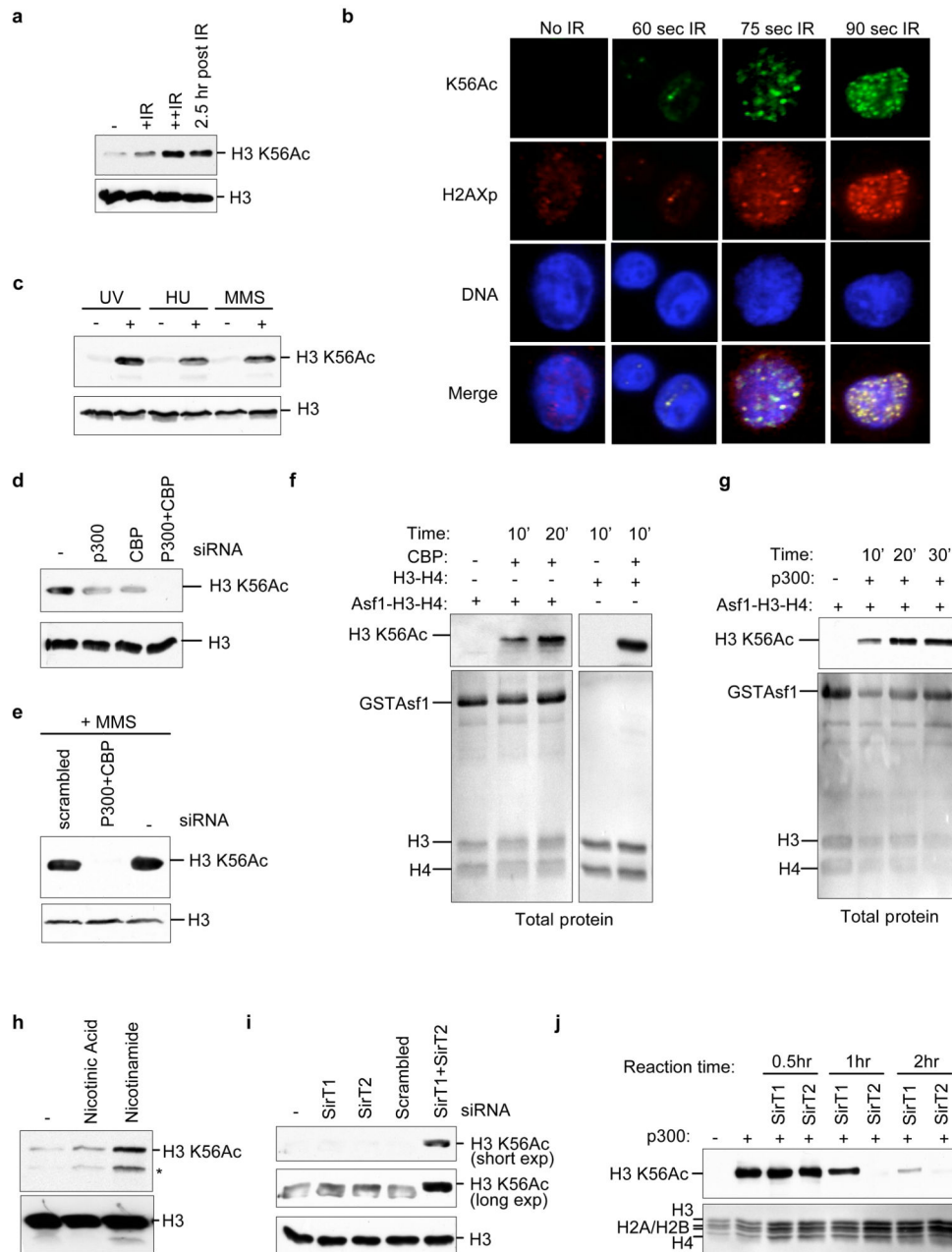


Figure 3. Human CBP/p300 acetylates H3 K56 while SirT1 and SirT2 deacetylate H3 K56Ac
a. Levels of H3 K56Ac on human chromatin following gamma irradiation. **b.** H3 K56Ac localizes to DNA damage foci. **c.** HU, MMS and UV induce H3 K56Ac. **d.** CBP/p300 are required for acetylation of H3 K56 in the absence and presence, **e.** of DNA damage. **f.** Human CBP and p300, **g.** acetylate H3 K56 in vitro. **h.** Inhibition of NAD-dependent HDACs increases H3 K56Ac levels. **i.** Human SirT2 and SirT1 deacetylate H3 K56Ac in vivo. **j.** Human SirT2 and SirT1 deacetylate H3 K56Ac in vitro.

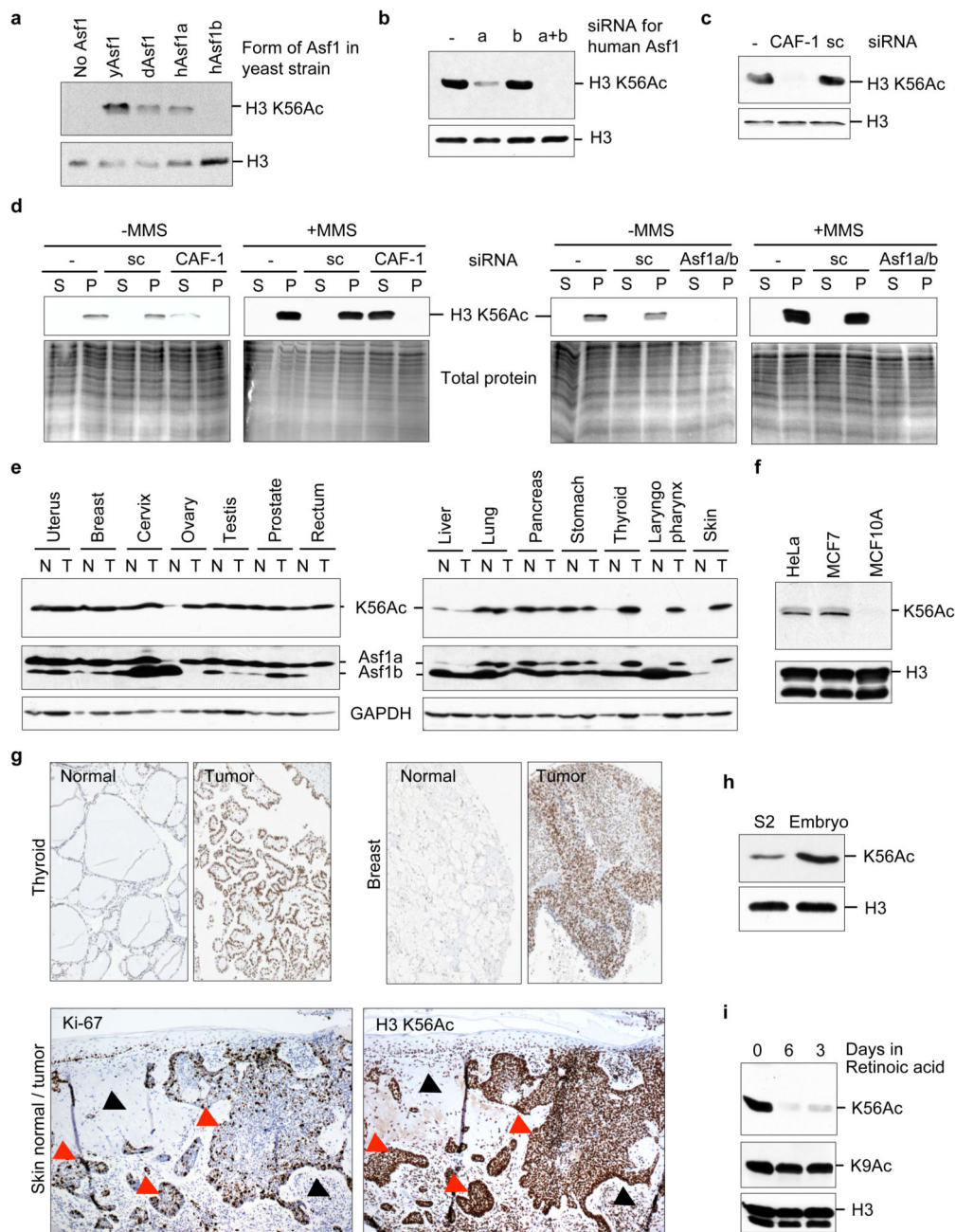


Figure 4. Asf1a drives K56 acetylation in human cells and tumors

a. Asf1a promotes K56 acetylation in yeast and humans (**b.**). **c.** and **d.** CAF-1 mediates H3 K56ac assembly onto chromatin. sc - scrambled siRNA. **e.** K56Ac and Asf1a correlate in matched normal (N) and tumor (T) pairs. **f.** Elevated K56Ac in tumorigenic cells and tumors (**g.**). Nuclei – blue; K56Ac - brown. Comparison of K56Ac and the proliferation marker Ki-67 in adjacent sections of late grade skin cancer. Red arrows - invading tumor. Black

arrows - normal tissue. **h.** *Drosophila* embryos have elevated K56Ac. **i.** Elevated K56Ac in undifferentiated cells.

Author Manuscript

Author Manuscript

Author Manuscript

Author Manuscript